

CHAPTER ONE HUNDRED FORTY SEVEN

UNIFORM LONGSHORE CURRENT MEASUREMENTS AND CALCULATIONS

P.J. Visser*

ABSTRACT

A description is given of laboratory experiments on uniform longshore currents and the comparison of the data with longshore current profiles predicted by a mathematical model. For the mathematical model it is assumed that longshore current generation takes place between the plunge line and the shoreline (instead of shoreward of the breaker line) and Battjes' (2,3) lateral friction model is applied. Good agreement between theory and laboratory data is achieved with realistic values of the bottom roughness.

1. INTRODUCTION

When waves break at an angle to the coast, a mean current is generated parallel to the shoreline (see fig. 1). This longshore current is confined to a zone with a width of order two times the width of the surf zone. Longshore currents and the associated transport of sediment play a significant role in the erosion and deposition of sediment and the dispersion of pollutants.

Since the introduction of the concept of radiation stresses by Longuet-Higgins and Stewart (15), the theory of longshore currents has progressed considerably: Bowen (4), Thornton (18), Longuet-Higgins (13), James (8), Battjes (1), Jonsson, Skovgaard and Jacobsen (10), Liu and Dalrymple (12). In these theories the equations of motion are averaged over the water depth and over the wave period. Then, in a steady state, there is a balance of the longshore driving force, the bottom frictional stress and the lateral friction. The theoretical achievements obtained by these authors are considerable, although some of the assumptions are rather crude, for instance concerning the eddy viscosity outside the surf zone, the dissipation of wave energy inside the surf zone and the bottom friction.

- Measurements of longshore current profiles were done, both
- in the field: in the Nearshore Sediment Transport Study, see Seymour and Gable (16), and in more detail
 - in the laboratory by Galvin and Eagleson (7) and Visser (20,21).

*Scientific Officer, Department of Civil Engineering, Delft University of Technology, P.O. Box 5048, 2600 GA Delft, The Netherlands.

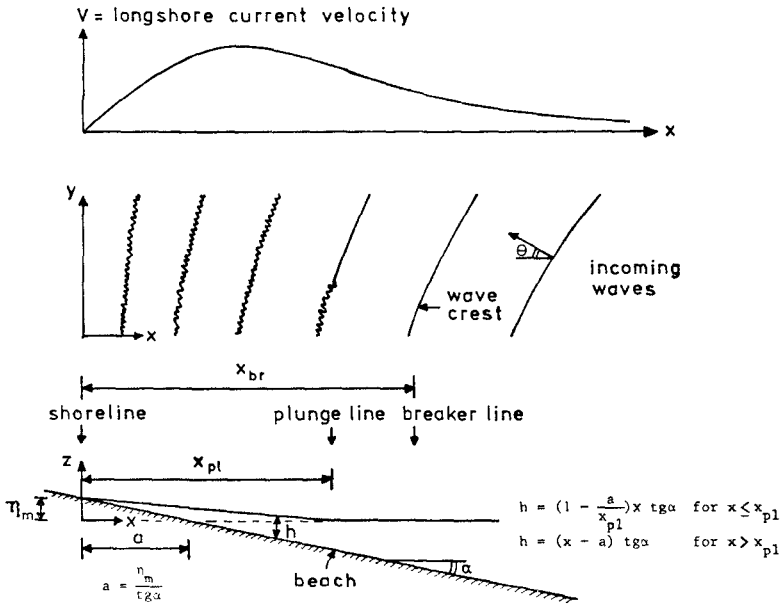


Fig. 1 - The nearshore region.

Care must be taken in comparing Galvin and Eagleson's measurement results with theoretical longshore current profiles, since the measured currents were not uniform along the coast which was caused by the wave basin geometry and the recirculation system.

The measured longshore current profiles, which are compared in this paper with an improved longshore current model, are all uniform along the coast as a result of the application of the method for the adjustment of the proper longshore current in a wave basin proposed by Visser (19), see also Visser (20). In this method the wave basin geometry and the proper recirculation flow through the longshore current openings in the wave guides are determined such that the circulation flow between the wave guides Q_c (see fig. 2) is minimal.

The aim of the present investigation is to get more insight into the dynamics of longshore current generation by sea waves, i.e. dissipation of wave energy (longshore driving force) and production of turbulence by breaking, diffusion of turbulence and momentum (lateral friction), bottom frictional stress. The principal objective is a mathematical model for calculations of longshore currents being more reliable than the existing ones. The basic assumptions are uniformity in longshore direction, steady state conditions and the bottom contours are straight and parallel to the beach. The investigation is restricted to regular waves.

The scope of the present study is the comparison of longshore currents measured in a wave basin with the current profiles predicted by a mathematical model. In the latter it is therefore assumed that the angle of the beach slope is constant and that the positions of the breaker line, the plunge line and the wave set-up line are known (i.e. following from the measurements). The breaker line is here defined as the line on which the wave height is maximal. The plunge line is the line where the curly crest of a plunging breaker impinges on the preceding wave trough (see also fig. 1).

In the present mathematical model the longshore driving force is modeled taking into account the physical fact that dissipation of wave energy takes place between the plunge line and the shoreline instead of in the whole surf zone (that is shoreward of the breaker line). The bottom friction is modeled by considering the combined orbital and current velocity vector. In fact it is still unclear how to combine the orbital and current velocity near the bottom. Therefore different bottom friction models are applied. The lateral friction is modeled according to Battjes (2,3): it is one of the aims of this investigation to examine the applicability of the ideas proposed by Battjes.

2. EXPERIMENTS

2.1 Experimental arrangement

The experiments were performed in the 16.60 x 34.00 m² wave basin of the Civil Engineering Department of the Delft University of Technology. Opposite to the snake-type wave generator smooth concrete beaches were constructed with slopes 1:10 (fig. 2) and 1:20 (fig. 3), respectively. For the last experiment the 1:20 slope was roughened by bonding 5 - 9 mm gravel with a thin grout on the smooth concrete. The wave guide walls were composed of concrete elements and installed at angles of 15.4 or 31.0 degrees with the normal to the wave board.

To approximate the longshore current flow generated by a uniform wave field on a straight infinitely long and uniform beach, a wave basin configuration was chosen with longshore current openings in both wave guides and with an external recirculation Q_r which is completely effected by a pump. A distribution system was built in the longshore current opening of the upstream wave guide in order to increase the length along which the longshore current is uniform. The recirculation flow Q_r was distributed in this system according to the expected distribution of the longshore current flow and was readjusted if that turned out to be necessary. The correct width of the longshore current opening in the downstream wave guide and the proper rate of recirculation flow were determined experimentally, i.e. followed from the application of an experimental method with which it is possible to obtain the uniform longshore current in the present wave basin geometry, (see Visser (20)).

2.2 Experimental procedure

The experimental procedure is given in table 1. Because of the rather fast spreading of dye in the breaker zone, it was not possible to follow the dye in this zone over distances exceeding about 1.0 m. In view of the accuracy, the number of observations per point was

measurements of	measuring method	sections (see fig.2 and 3)	hor. distance between two measuring points	number of observations/ observational time
velocity	dye ($KMnO_4$), in the vertical in 3 points (surface, mid-depth ⁽¹⁾ , bottom)	0, 1, 2, 3, 4	1:10 slope 0.20 m ⁽³⁾ 1:20 slope 0.40 m	surf zone: 20 ⁽⁴⁾ } outside } surf zone: 10 }
wave height	resistance wave probes	1, 2	0.20 m	90 seconds
breaker height and position		a, b, c, d, e	0.20 m (20 points per section)	
		3-5 sections on and near the breaker line ⁽²⁾	0.20 m (29 points per section)	
mean water level	static head in pots connected with tappings flush- mounted in the beach	1, 2	1:10 slope 0.20 m 1:20 slope 0.40 m (in the surf zone also in intermediate points)	
angle of incidence	wave probes photograph	constant depth part of the basin breaker line		about 10 about 20
position of plunge line	visually	near 1 and 2		6

(1) except near the water line (2) near the middle of the beach (3) 0.20 m near the water line
(4) i.e. 60 observations give a depth-averaged longshore current velocity (40 near the water line)

Table 1 - Experimental procedure.

enlarged to 20 and the measurements were conducted by two persons in this zone. Outside the surf zone, the spreading of dye was rather small and there the measured excursion time of dye was at least 3 seconds (and the excursion distance was 0.30 m or 0.50 m).

exp nr.	beach	$\tan \alpha$	T sec	d_1 cm	θ_1 degr	H_1 cm	H_0 cm	θ_0 degr	H_{br} cm	d_{br} cm	θ_{br} degr	η_m cm	x_{br} cm	p	breaker type
1	smooth	0.101	2.01	39.9	31.1	7.2	9.8	61.5	10.5	10.4	20.9	4.20	145	0.59	pl.
2	smooth	0.101	1.00	39.9	30.5	9.5	10.2	32.5	10.0	10.9	24.0	2.78	136	0.57	pl.
3	smooth	0.101	1.00	40.1	15.4	8.9	9.6	16.4	9.7	11.4	12.1	2.75	141	0.60	pl.
4	smooth	0.050	1.02	35.0	15.4	7.8	8.5	17.0	9.1	11.0	12.5	1.64	251	0.76	pl.
5	smooth	0.050	1.85	34.8	15.4	7.1	7.5	26.4	10.8	11.8	11.5	2.45	279	0.75	pl.
6	smooth	0.050	0.70	35.0	15.4	5.9	6.0	15.5	5.8	8.8	14.3	1.00	194	0.82	sp./pl.
7	smooth	0.050	1.02	35.0	15.4	7.8	8.5	17.0	9.0	12.2	12.2	1.64	275	0.78	pl.

Table 2 - Beach and wave field properties and quantities; the indices 0,1 and br refer to values on deep water, constant depth of the basin and the breaker line, respectively.

2.3 Experimental results

Seven experiments were performed, see table 2 (α = slope angle, T = wave period). The results of the measurements of wave heights (H), angles of incidence (θ), (still water) breaker depth (d_{br}), maximum wave set-up (η_m), positions of the breaker line (x_{br}) and the plunge line ($p = x_{pl}/x_{br}$) with respect to the shoreline ($x = 0$), and breaker types are also listed in table 2, see also fig. 1. The wave height and the angle of incidence on deep water were calculated from the measured values on constant depth part of the basin using linear wave theory and Snell's law.

The results of the mean water level measurements, see Visser (21), indicate clearly that the wave set-up starts at the plunge line instead of the breaker line. This is in conformity with experimental results of other investigators, for instance Bowen, Inman and Simmons (5). Consequently the transfer of momentum from waves to wave set-up and longshore current takes place shoreward of the plunge line, instead of shoreward of the breaker line in the whole surf zone, as often assumed. The mean water level measurements show further that the gradient of the wave set-up is more or less constant, as often observed on slopes with comparable steepnesses. The results of the wave height measurements in sections 1 and 2 indicate that in the breaker zone the wave height remains more or less proportional to the mean water depth, see Visser (21); this is also in agreement with other measurements on comparable slopes.

From the measured current velocities in three points per vertical, the depth-averaged current velocity in that vertical has been calculated. The depth-averaged longshore current velocities in the different sections have been given the present uniform longshore current profiles in the

sections 0,1,2 and 3 (experiments 1,2,3,4 and 7) and in the sections 0,1 and 2 (experiments 5 and 6). The uniformity of these longshore current profiles of each of the seven experiments is very satisfactory, see Visser (20); examples are given in fig. 4 (experiment 2) and fig. 5 (experiment 4). The depth-averaged and longshore-averaged measured current velocities are given in chapter 4 in combination with computed longshore current profiles.

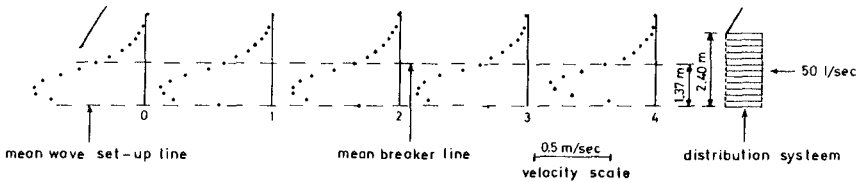


Fig. 4 - Depth-averaged uniform longshore current velocities in experiment 2.

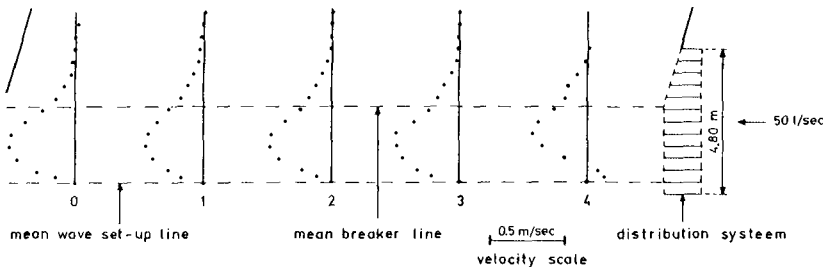


Fig. 5 - Depth-averaged uniform longshore current velocities in experiment 4.

As already described in Visser (19,20), the systematic error of the current velocity measurements is small (order 1%). The random error of the measured velocity in a point (following from 10 or 20 readings) is about $\pm 4\%$ for the measurements in and near the surf zone. This gives for the depth-averaged velocity in this zone a random error of $\pm 2.5\%$. In view of the measuring technique (dye), both the systematic and random error are surprisingly small.

3. MATHEMATICAL MODEL

The equation of motion in longshore direction for the situation under consideration can be written as

$$\frac{dS_{xy}}{dx} - \frac{d}{dx} \left\{ \rho \mu_m h \frac{dV}{dx} \right\} + \tau_{by} = 0, \tag{1}$$

in which

$$\frac{dS_{xy}}{dx} = \frac{\sin \theta}{c} \frac{dF_x}{dx} = - \frac{\sin \theta}{c} D = \text{longshore driving force}, \tag{2}$$

$$\frac{\sin \theta}{c} = \text{constant according to Snell's law (c = phase velocity)}, \tag{3}$$

F_x = flux of wave energy normal to the coast per unit length of shoreline,

D = local rate of wave energy dissipation,

x, y = coordinates in offshore, longshore direction, respectively,

μ_m = eddy viscosity (momentum),

h = mean water depth, V = longshore current velocity,

τ_{by} = mean bottom frictional stress in y-direction.

3.1 Longshore driving force

If it is assumed that for $x \leq x_{br}$

1. the wave height is proportional to the mean water depth,
2. the gradient of the wave set-up is constant,
3. the shallow water approximation of linear wave theory can be used and
4. the dissipation of wave energy takes place shoreward of the breaker line,

then the following simple model for D , see Battjes (2), can be derived

$$D = \begin{cases} 0 & \text{for } x > x_{br}, \end{cases} \tag{4}$$

$$D = \begin{cases} \propto x^{3/2} & \text{for } x \leq x_{br}. \end{cases} \tag{5}$$

The assumptions 1 and 2 are in agreement with the present observations. For the present model it is assumed that

1. the dissipation of wave energy takes place for $x \leq x_{p1} = px_{br}$,
2. D is proportional to $x^{3/2}$ for $x \leq x_{p1}$, $D = 0$ for $x > x_{p1}$,
3. the transport of wave energy towards the shore = the transport of wave energy in x-direction on deep water given by linear wave energy =

$$(F_x)_o = \frac{1}{2} E_o c_o \cos \theta_o, \tag{6}$$

where $E_0 = \frac{1}{8} \rho g H_0^2$ = wave energy on deep water per unit area.

Then it follows from eq. (2) that:

$$\frac{dS_{xy}}{dx} = - \underbrace{\frac{1}{4} E_0 \sin 2\theta_0}_I \cdot \underbrace{\frac{5}{2} \frac{x}{x_{pl}^{5/2}}}_{II} \quad \text{for } x \leq x_{pl} \quad (7)$$

The first part (I) of eq. (7) is the lateral thrust exerted by the waves on the longshore current. As emphasized by Longuet-Higgins (14), the expression for this total lateral thrust is exact and does not depend on the application of small amplitude theory to waves in the longshore current zone. The second part (II) of eq. (7) denotes the distribution of the lateral thrust across the region in which dissipation of wave energy takes place.

3.2 Bottom frictional stress

For the combination of a wave field and a mean current in y-direction, the mean bottom friction in longshore direction can be expressed, see Visser (21), as:

$$\tau_{by} = C \rho V^2 f(\theta, \xi \frac{u_m}{V}), \quad (8)$$

where

$$f(\theta, \xi \frac{u_m}{V}) = \frac{1}{T} \int_0^T \{1 + 2 \xi \frac{u_m}{V} \sin \theta \cos \omega t + (\xi \frac{u_m}{V})^2 \cos^2 \omega t\}^{\frac{1}{2}} \times \\ \times (1 + \xi \frac{u_m}{V} \sin \theta \cos \omega t) dt, \quad (9)$$

C = a dimensionless bottom friction coefficient,

u_m = maximum orbital velocity near the bottom,

ξ = a dimensionless factor which depends on how the orbital and mean current velocity near the bottom are combined.

If the orbital velocity near the bottom and the depth-averaged longshore current velocity are combined then $\xi = 1$. Bijker (6) has proposed to combine the horizontal orbital and current velocity vector in the (hypothetical) boundary layer and arrives at (8) with (9) in which

$$\xi_B = \frac{p' \kappa}{\sqrt{C}} \approx \frac{0.16}{\sqrt{C}} \quad (p' \approx 0.4), \quad (10)$$

$$\text{where } C = \left(\frac{\kappa}{\ln \frac{12h}{r}} \right)^2, \quad (11)$$

with r = diameter of the bottom roughness elements,
is Nikuradse's expression for C for rough turbulent flow.
Bijker's model has been modified by Swart (17):

$$\xi_s = \sqrt{\frac{C'}{C}} = \left[\frac{0.5}{C} \exp \{ - 5.977 + 5.213 \left(\frac{r}{a_b} \right)^{0.194} \} \right]^{\frac{1}{2}}, \quad (12)$$

in which C' corresponds with Jonsson's (9) wave friction factor
and a_b = amplitude of water particle excursion near the bottom.
For a linear wave theory is applied: this is justified as demonstrated
by Lemchauté, Divoky and Lin (11).

3.3 Lateral friction

The eddy viscosity is modelled according to Battjes (2):

$$\mu_m = M q l, \quad (13)$$

in which

M = constant of order 1,

q = characteristic turbulent velocity,

l = characteristic length of turbulence (is set equal to h). (14)

The turbulent velocity is calculated from Battjes' (3) balance of
turbulent energy

$$\rho h \epsilon - \frac{d}{dx} \left\{ \mu_e h \frac{d(\frac{1}{2} \rho q^2)}{dx} \right\} = D, \quad (15)$$

where

ϵ = q^3/h = mean rate of turbulent energy dissipation per unit mass, (16)

D = local rate of wave energy dissipation which is set equal to the
rate of production of turbulent energy,

μ_e = eddy viscosity (energy) which is set equal to μ_m .

Battjes (3) gives a local solution of eq. (15) in the neighbourhood of
the plunge line as defined in this paper. It is, however, possible to
give a complete analytical solution, see also Visser (21). Substitution
of (13), (14), (16) and the expressions for h (given in fig. 1) into (15)
leads to a differential equation with the following solution

$$q = \left\{ A_1 \left(\frac{x}{x_{p1}} \right)^{r_1} + \frac{D}{\rho} \right\}^{1/3} \quad \text{for } x \leq x_{p1}, \quad (17)$$

$$q = \left\{ A_2 (x - a)^{r_2} \right\}^{1/3} \quad \text{for } x > x_{p1}, \quad (18)$$

in which

$$A_1 = \frac{(x_{p1} - a) \left(\frac{dD}{dx}\right)_{p1} - r_2 D_{p1}}{\rho (r_2 - r_1) \left(1 - \frac{a}{x_{p1}}\right)}, \quad A_2 = \frac{(x_{p1} - a)^{-r_2} \{x_{p1} \left(\frac{dD}{dx}\right)_{p1} - r_1 D_{p1}\}}{\rho (r_2 - r_1)}, \quad (19)$$

$$r_1 = -0.5 + 0.5 (1 + 4B_1)^{\frac{1}{2}}, \quad r_2 = -0.5 - 0.5 (1 + 4B_2)^{\frac{1}{2}}, \quad (20)$$

$$B_1 = B_2 \left(1 - \frac{a}{x_{p1}}\right)^{-2}, \quad B_2 = 3M^{-1} \text{tg}^{-2} \alpha, \quad (21)$$

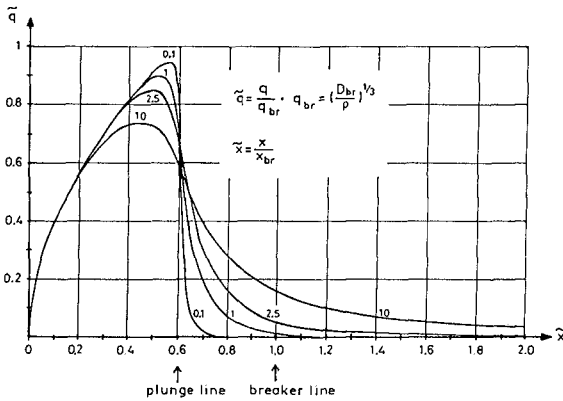


Fig. 6 - Calculated dimensionless turbulent velocity \tilde{q} as function of \tilde{x} for different M (applicable to experiment 3).

As example, fig. 6 shows the theoretical \tilde{q} for different M applicable to experiment 3.

3.4 Numerical model

Substitution of (7), (8) and (13) into (1) yields a second order non-linear differential equation which has to be solved numerically, see Visser (21). Because of the non-linearity, this has been done with an iteration procedure.

The boundary conditions are $V = 0$ at $x = 0$ and $V = 0$ as $x \rightarrow \infty$. Since for $x > 2 x_{br}$ the longshore current velocity V becomes very small, the boundary condition at $x \rightarrow \infty$ has been rewritten as $V =$ measured value at $x \approx 2.5 x_{br}$.

The numerical program has been checked with the aid of an analytical solution which can be derived for $p = 1$, $\theta =$ small and $\xi u_m/V =$ large.

4. COMPARISON OF MEASURED AND COMPUTED LONGSHORE CURRENTS

The rate of agreement between measured and computed longshore currents can be influenced by the choice of two coefficients in the mathematical model, i.e. the bottom friction coefficient C (through the diameter r of the roughness elements) and the lateral friction coefficient M . This is justified to a certain extent because r and M are not (exactly) known. But it is to be expected that

for the smooth slopes : $r \approx 0.001$ m ($C \approx 0.003$),

for the rough slope : $r \approx 0.01$ m ($C \approx 0.008$).

Further Battjes' (2,3) lateral friction coefficient M is expected to be of order 1.

The smooth concrete slopes 1:10 and 1:20 were constructed with the same materials, but in principle it is possible that the roughnesses of both slopes differ slightly due to 1) a small difference in workmanship and 2) the fact that the present measurements on the 1:10 slope have been preceded by other experiments on the same slope while the 1:20 slope was constructed especially for the present experiments (the roughness of a concrete slope increases generally in time).

In principle it is also possible to vary the factor p and to influence in this way the rate of agreement between measured and computed longshore currents; the computations, however, have been carried out with the measured value of p , see table 2.

The rate of agreement between measured and computed longshore current profiles, has been expressed in a standard deviation, see Visser (21). Thus, optimal values for M and r have been determined and the validity of the different bottom friction models (i.e. different expressions for ξ) for the present application has been judged.

From the rate of agreement computations it follows that

- $M \approx 2.5 - 3.0$, which is indeed of order 1,
- both $\xi = 1$ and $\xi = \xi_s$ give good agreement between measured and computed longshore current profiles with realistic values of r ; the general agreement obtained with ξ_s is somewhat better than with $\xi = 1$,
- the agreement between measured and computed longshore current is very poor with $p = 1$.

Figures 7 and 8 show the measured and computed longshore current profiles of the seven experiments; these computed longshore current profiles are based on $\xi = \xi_s$, and further on $M = 3.0$, $r = 0.0012$ m for the smooth concrete 1:10 slope, $r = 0.0004$ m for the smooth concrete 1:20 slope and $r = 0.005$ m for the rough 1:20 slope. The agreement between measurements and theory is satisfactory, even very good in experiments 1 through 5, but less in experiments 6 and 7. The longshore current velocities in experiments 6 and 7 are smaller than in the other experiments: the less good agreement between measured and computed longshore current profiles in these experiments is probably caused by the fact that due to $\xi = \xi_s$ in eq. (8) the bottom friction is over-estimated in the weak current situation, as it is also the case with $\xi = \xi_b$, see Visser (21).

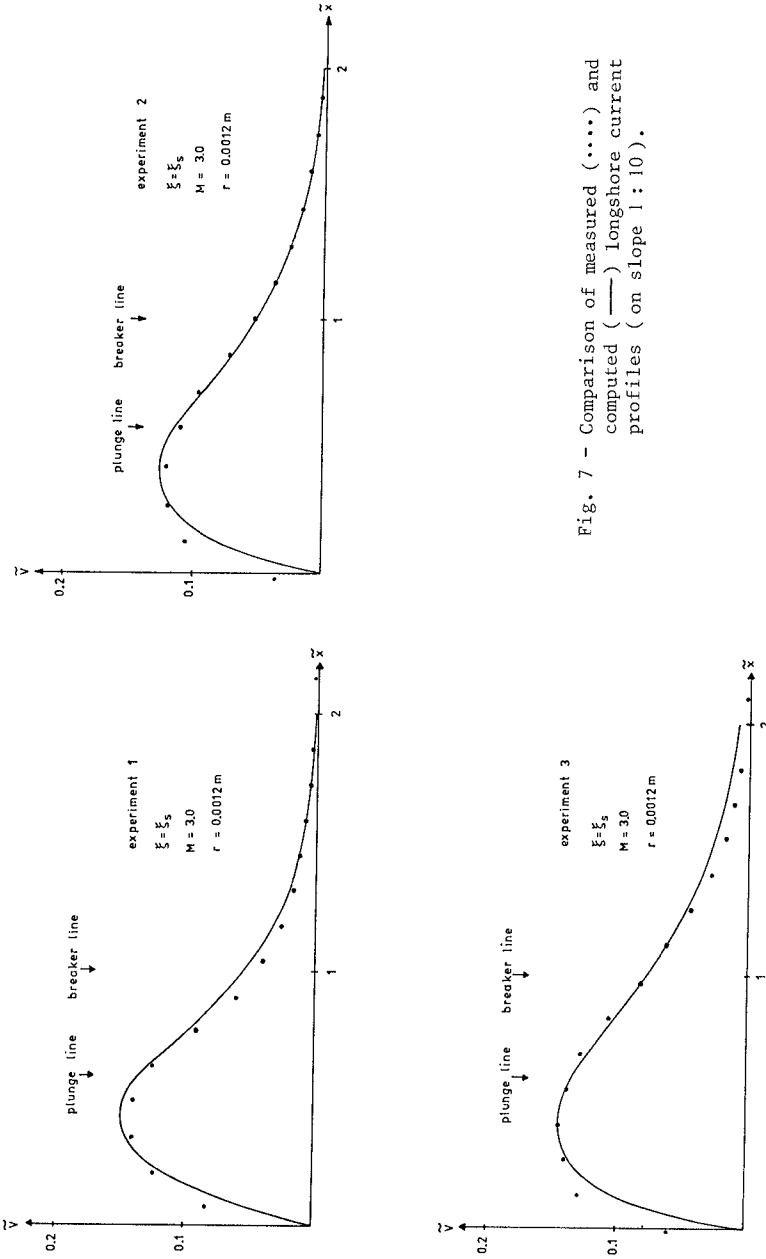


Fig. 7 - Comparison of measured (••••) and computed (—) longshore current profiles (on slope 1 : 10).

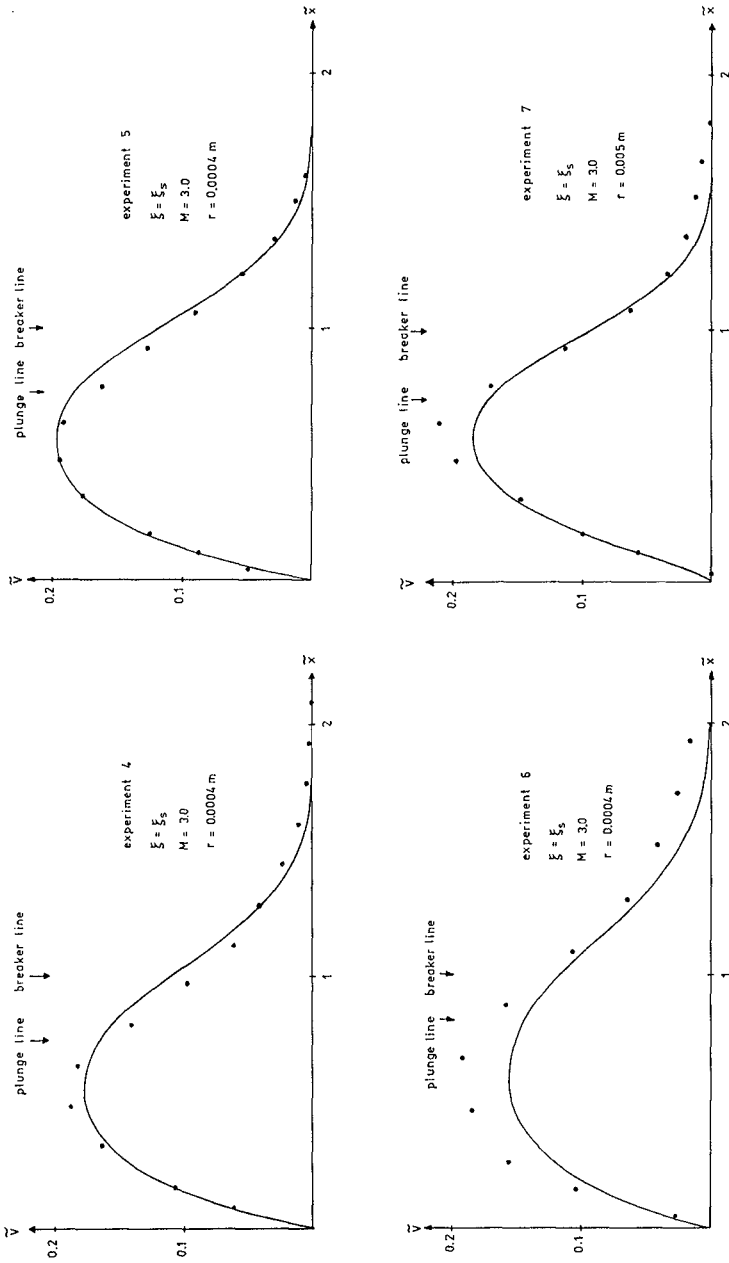


Fig. 8 - Comparison of measured (.....) and computed (——) longshore current profiles (on slope 1 : 20).

5 DISCUSSION AND CONCLUSIONS

The proposed mathematical longshore current model is more plausible on physical grounds than earlier models, in particular the formulation of the longshore driving force (action of this force shoreward of the plunge line) and the application of Battjes' (2,3) lateral friction model (in which the relevant properties of the horizontal turbulent momentum exchange are estimated taking account of the wave energy dissipation by breaking). This mathematical longshore current model has been verified by a number of longshore current measurements in a wave basin. The experimental set-up and execution has been extremely careful in order to obtain reliable results.

The conclusions from this investigation can be summarized as follows:

1. The data obtained from the present longshore current experiments are very usable to check the theoretical results: the rate of accuracy of the measurement results is high, the longshore current profiles are uniform and these were measured in detail.
2. The agreement between the longshore currents predicted by the mathematical model and the experiments is good. This good agreement has been achieved by using realistic values of the bottom roughness.
3. The present investigation confirms the utility of Battjes' (2,3) lateral friction model: best results have been achieved with $M \approx 2.5-3.0$, which is indeed of order 1.
4. The longshore current generation takes place between the plunge line and the shoreline (in plunging breakers), instead of in the whole breaker zone.
5. Bottom friction models in which the orbital and mean current velocity are combined, with a depth-dependent bottom friction coefficient and with $\xi = 1$ or $\xi = \xi_s$ can be used for the present application.

With respect to the last conclusion it is remarked that more research on this field is necessary because of the uncertainties regarding the real friction in case of combination of wave and current.

REFERENCES

1. BATTJES, J.A., 1974, Computation of set-up, longshore currents, run-up and overtopping due to wind-generated waves, Comm. on Hydraulics, Dep. of Civil Eng., Delft Univ. of Techn., Rep. no. 74-2, 244 pp.
2. BATTJES, J.A., 1975, Modeling of turbulence in the surf zone, Symposium on Modeling Techniques, California, 1975, A.S.C.E., New York, pp. 1050-1061.
3. BATTJES, J.A., 1983, Surf zone turbulence, Proc. Seminar on Hydrodynamics of waves in coastal areas, I.A.H.R., Moscow, 1983, 4 pp.
4. BOWEN, A.J., 1969, The generation of longshore currents on a plane beach, J. Mar. Res., vol. 27, pp. 206-215.
5. BOWEN, A.J., INMAN, D.L. and SIMMONS, V.P., 1968, Wave "set-down" and set-up, J. Geoph. Res., vol. 73, pp. 2569-2577.

6. BLIJKER, E.W., 1967, Some considerations about scales for coastal models with movable bed, Delft Hydr. Lab., Publ. no. 50, 142 pp.
7. CALVIN, C.J. and EACLESON, P.S., 1965, Experimental study of long-shore currents on a plane beach, U.S. Army Coastal Eng. Res. Center, Tech. Mem. 10, Washington, D.C., 60 pp.
8. JAMES, I.D., 1972, Some nearshore effects of ocean waves, Univ. of Cambridge, Cambridge, diss., 130 pp.
9. JONSSON, I.C., 1967, Wave boundary layers and friction factors, Proc. 10th Conf. Coastal Eng., Tokyo, 1966, pp. 127-148.
10. JONSSON, I.C., SKOVGAARD, O. and JACOBSEN, T.S., 1975, Computation of longshore currents, Proc. 14th Conf. Coastal Eng., Copenhagen, 1974, pp. 699-714.
11. LEMEAUTE, B., DIVOKY, D. and LIN, A., 1969, Shallow water waves: a comparison of theories and experiments, Proc. 11th Conf. Coastal Eng., London, 1968, pp. 86-107.
12. LIU, P.L-F. and DALRYMPLE, R.A., 1978, Bottom frictional stresses and longshore currents due to waves with large angles of incidence, J. Mar. Res., vol. 36, pp. 357-375.
13. LONGUET-HICCINS, M.S., 1970, Longshore currents generated by obliquely incident sea waves, J. Geoph. Res., vol. 75, pp. 6778-6801.
14. LONGUET-HIGGINS, M.S., 1972, Recent progress in the study of long-shore currents, in "Waves and Beaches", ed. by R.E. Meyer, Academic Press, New York, pp. 203-248.
15. LONGUET-HICCINS, M.S. and STEWART, R.W., 1964, Radiation stresses in water waves: a physical discussion with applications, Deep-Sea Res., vol. 11, pp. 529-562.
16. SEYMOUR, R.J. and CABLE, C.C., 1981, The Nearshore Sediment Transport Study Field Investigations, Proc. 17th Conf. Coastal Eng., Sydney, 1980, pp. 1402-1415.
17. SWART, D.H., 1974, Offshore sediment transport and equilibrium beach profiles, Delft Hydr. Lab., Publ. no. 131, 217 pp.
18. THORNTON, E.B., 1969, Longshore current and sediment transport, Techn. Rep. 5, Dep. of Coastal and Oceanogr. Eng., Univ. of Florida, Gainesville, Florida, 171 pp.
19. VISSER, P.J., 1981, Longshore current flows in a wave basin, Proc. 17th Conf. Coastal Eng., Sydney, 1980, pp. 462-479.
20. VISSER, P.J., 1982, The proper longshore current in a wave basin, Comm. on Hydraulics, Dep. of Civil Eng., Delft Univ. of Techn., Rep. 82-1, 86 pp.
21. VISSER, P.J., 1984, A mathematical model of uniform longshore currents and the comparison with laboratory data, Comm. on Hydraulics, Dep. of Civil Eng., Delft Univ. of Techn., Rep. 84-2.